Fabrication of particular structures of hexagonal boron nitride and boron-carbon-nitrogen layers by anisotropic etching

Riteshkumar Vishwakarma, Subash Sharma, Sachin M. Shinde, Kamal P. Sharma, Amutha Thangaraja, Golap Kalita, Masaki Tanemura

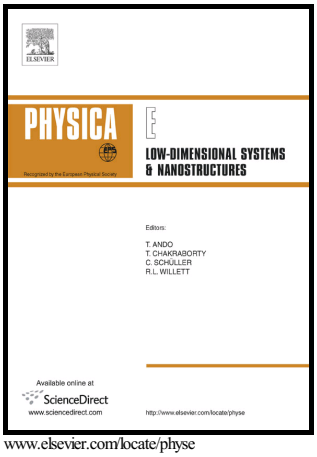

www.elsevier.com/locate/physe

PII: S1386-9477(15)30309-X
DOI: http://dx.doi.org/10.1016/j.physe.2015.12.004
Reference: PHYSE12229

To appear in: *Physica E: Low-dimensional Systems and Nanostructures*

Received date: 8 October 2015
Revised date: 4 December 2015
Accepted date: 10 December 2015

Cite this article as: Riteshkumar Vishwakarma, Subash Sharma, Sachin M Shinde, Kamal P. Sharma, Amutha Thangaraja, Golap Kalita and Masak Tanemura, Fabrication of particular structures of hexagonal boron nitride an boron-carbon-nitrogen layers by anisotropic etching, *Physica E: Low dimensional Systems and Nanostructures* http://dx.doi.org/10.1016/j.physe.2015.12.004

Fabrication of particular structures of hexagonal boron nitride and boron-carbon-nitrogen layers by anisotropic etching

Riteshkumar Vishwakarma, Subash Sharma, Sachin M. Shinde, Kamal P. Sharma, Amutha Thangaraja, Golap Kalita*, Masaki Tanemura

Department of Frontier Materials, Nagoya Institute of Technology, Gokiso-cho, Showa-ku, Nagoya 466-8555, Japan

Corresponding Author: *E-mail: kalita.golap@nitech.ac.jp (G.K.); Phone/Fax: +81-527355216

Abstract:

Anisotropic etching of hexagonal boron nitride (h-BN) and boron-carbon-nitrogen (BCN) basal plane can be an exciting platform to develop well-defined structures with interesting properties. Here, we developed an etching process of atomically thin h-BN and BCN layers to fabricate nanoribbons (NRs) and other distinct structures by annealing in H_2 and Ar gas mixture. BCN and h-BN films are grown on Cu foil by chemical vapor deposition (CVD)

using solid camphor and ammonia borane as carbon, nitrogen and boron source, respectively. Formation of micron size well-defined etched holes and NRs are obtained in both h-BN and BCN layers by the post growth annealing process. The etching process of h-BN and BCN basal plane to fabricate NRs and other structures with pronounced edges can open up new possibilities in 2D hybrid materials.

Keywords: Anisotropic etching; hexagonal boron nitride; boron-carbon-nitrogen; nanoribbons

1. Introduction

Anisotropic etching is an important tool for microfabrication processes, creating distinct microscopic features. These microstructures obtained by anisotropic etching are commonly used for nanoelectronic devices, thereby achieving desired optical, electrical, and physical properties [1,2]. The development of various two dimensional (2D) materials in the last decade has attracted significant attention for electronic device applications [3-5]. In this prospect, achieving anisotropic etching of 2D materials can be one of the most important aspect for nanoelectronics. Anisotropic etching of graphite sheet, exfoliated few-layer graphene and chemical vapor deposited graphene has been significantly explored to obtain regular, well-defined zigzag or armchair edge structures [6-11]. Anisotropic etching of

graphene basal plane has been achieved with metal catalytic nanoparticles in presence of H_2, selective oxidation, and water vapor at an elevated temperature [9-13]. The etching process enable to fabricate nanoribbons with particular edge structures of high quality graphene. Similarly, creating hexagonal hole in graphene with pronounced edges by the etching process also provide a platform to fabricate in-plane heterostructure with other 2D materials [14,15].

In contrast to previous reports, anisotropic etching of h-BN and BCN film is not addressed for possibilities of fabricating NRs or other regular structures. Very recently, we demonstrate possibility of opening triangular holes in triangular h-BN crystals by anisotropic etching [16]. h-BN is an insulating layered material consisting of sp^2 hybridized alternating B and N atoms with similar honeycomb lattice of graphene [17,18]. Monolayer and few-layer h-BN have been derived by exfoliation and chemical vapor deposition (CVD) synthesis process for field effect transistor (FET) applications [17,19-22]. Previously, theoretical analysis has predicted that the basic properties of h-BN can be changed by incorporating graphene in the h-BN lattice with an ordered structure [23-25]. Developing heterostructures with controlled shape, size and edges can introduce unexpected electronic and magnetic properties [25]. Further, it has been predicted that atomically thin h-BN NRs

can exhibit narrow band gap with improved conductivity owing to transverse electric field or edge structures [26,27]. Similarly, half-metallicity in BCN NRs has been expected by theoretical analysis [28]. Till date, the only way to derive h-BN NRs is unzipping of nanotubes, while synthesis of BCN NRs is much more challenging [29,30]. The unzipping process of nanotubes has inevitable issues in precisely controlling the edge structures, width, number of layers and defects formation. In this work, we have developed an anisotropic etching process of atomically thin h-BN and BCN film to overcome the challenges for NRs fabrication. The anisotropic etching process can be very simple and effective approach to fabrication well-defined NRs with control width and length for nanoelectronic and spintronic applications.

2. Experimental

BCN and h-BN films were synthesized on Cu foil with and without mixing camphor (C source) and ammonia borane (Borazane; H_3NBH_3) (N and B source) in an atmospheric pressure chemical vapor deposition (APCVD) method, respectively [16]. h-BN and BCN layered materials were obtained on 25 μm Cu foil for a growth duration of 30 min. We explore anisotropic etching process of the as-synthesized continuous h-BN and BCN film on Cu foil by annealing at 1020 ^{0}C in presence of Ar:H_2 gas mixture. A gas mixture of 85

sccm (standard cubic centimeters per minute) of Ar and 2.5 sccm of H_2 was used in these experiments (details in supplementary information, Figure S1). Synthesized and etched samples were analyzed by optical microscopy, field-emission scanning electron microscope (FE-SEM), auger electron spectroscopy (AES) and X-ray photoelectron spectroscopy (XPS) and Raman studies. Optical microscopy studies were carried out with VHX-500 digital microscope. FE-SEM analysis was performed using the JEOL JSM-7800F. XPS analysis was performed by VersaProbe using a monochromated Al Kα excitation source (1486.6 eV) to investigate the B and N concentration. Composition of the h-BN film was also analyzed by AES analysis using JAMP-7800 Auger microscope. Raman analysis of BCN film was carried out by NRS 3300 laser Raman spectrometer with a laser excitation energy of 532.08 nm.

3. Results and discussions

Figure1a-b shows optical microscope images of as-synthesized h-BN film on Cu foil. The h-BN films were grown by the APCVD technique using H_3NBH_3 as solid precursor. Monolayer and few-layers triangular h-BN crystals can be synthesized on Cu foil controlling the growth parameters of CVD process. Subsequently, continuous h-BN films are obtained on Cu foil increasing the growth duration. Figure 1a shows an optical

microscope image of the synthesized h-BN film. Several voids are observed with incomplete growth merging of the domains. Figure 1b shows an optical microscope image of complete Cu foil coverage with a continuous h-BN layer. The lateral size of individual h-BN crystals increases with longer growth duration, which finally merged together to form a continuous film. Elementary analysis was performed to measure the B and N ratio to confirm the h-BN film growth on Cu foil by XPS analysis. Figure 1c shows XPS B1s core level spectra with a peak-center at 192.3 eV, corresponding to binding energy of B. Similarly, figure 1d shows XPS N1s spectra with a peak-center at 400.1 eV, corresponding to N binding energy. AES analysis was also performed to confirm presence of B and N atoms and thereby growth of h-BN. Figure 1e shows the AES spectra of as-synthesized h-BN film on Cu foil. The AES analysis confirmed presence of B and N peaks with peak centers at 169 and 380 eV, respectively. These results clearly indicate growth of h-BN film on Cu surface by the AP-CVD technique using H_3NBH_3 as precursor. Etching process of synthesized h-BN film on Cu foil was explored with annealing in H_2 and Ar gas mixture at 1020 ^{0}C annealing temperature.

Figure 2a shows an FE-SEM image of etched h-BN film consisting of etched strips and triangular holes. The h-BN film etched to form various flakes and ribbon-like structures, as

well as triangular holes in individual flakes. The etched holes within the same h-BN flake possess almost identical size and edge orientation. The size of an individual triangular hole in around 1μm, which can enhance with annealing duration. It has been also observed that the orientation of triangular holes in different h-BN flakes can be completely opposite (supplementary materials, figure S2). The different orientation of the triangular holes may be due to opposite orientation of originally grown h-BN triangular crystals. Thus, the formation of etched hole is also significant to determine nature and orientation of h-BN crystals of a uniform continuous film. Again, the orientation also can be completely opposite to each other depending on the B and N terminated edges of individual triangular holes [16]. Edges of etched h-BN is quite pronounced and straight an important aspect of the etching process. We can observe a nanoparticle at the end of the etched strip, which turn at an angle (~65^0) as shown by the red arrow mark. Elementary analysis was performed of the nanoparticle comparing with h-BN coated Cu surface as shown in figure 2b. The analysis confirms presence of a SiO_2 nanoparticle. The SiO_2 nanoparticles get incorporated in the h-BN film on Cu foil during the growth process from the quartz tube of CVD. Effect of SiO_2 nanoparticles in h-BN crystals growth is not confirmed in this studies. Our findings provide interesting information regarding the etching behaviour of the h-BN basal plane.

Figure 2c shows an FE-SEM image of h-BN ribbon formation with the anisotropic etching process. The width of the ribbon is around 144 nm, as confirmed from the FE-SEM image. The NRs obtained by the etching process are connected to the original h-BN sheet or found individually on the substrate. Similarly, Figure 2d also shows ribbon like structure at another part of the sample, the etched ribbon structure is almost similar to that of graphene nanoribbon obtained by similar process. Width of the ribbon at one end is ~440 nm, whereas at the other end is around ~170 nm. Edges of the NRs are distinctive without any deformation or roughness. Figure 2e shows an optical microscope image of the transferred h-BN etched sample onto SiO_2/Si substrate. The ribbon-like structure and etched holes in the h-BN sheet are also visible after transferring without any deformation. At present the width of atomically thin individual h-BN NRs significantly varies depending on the extent of etching. As observed by Zeng et al, the h-BN NRs most favourably can be consisting of N-terminated zigzag edge structures [24]. Theoretically, it has been predicted that the bare zigzag BN NRs are electrically conductive and tunable band gap [23]. In such background, this can be a fascinating prospect to fabricate h-BN NRs and other well-defined structures by the developed etching process.

Similarly, BCN films were synthesized using mixture of camphor and ammonia borane solid precursors as C, N and B source, respectively. Mixture of such solid sources is a simple and alternative way to gaseous CVD process for obtaining different composition of layered materials. The vapour pressure and boiling point of the two precursors are different to each other, hence the sublimation temperature of precursors was controlled precisely during the growth process. Domain like structures and continuous films were obtained on Cu foil (supplementary materials, figure S3). The composition and incorporation of B and N atoms in the synthesized material was investigated by XPS analysis. Figure 3a shows a C1s XPS peak with peak center at 284.4 eV of the synthesized materials. At the same time, we observed less intense N and B peaks along with C peak. Figure 3b-c shows B1s and N1s XPS spectra with peak centers at around 191.2 and 398.3 eV, respectively. The observation of B and N along with C atoms indicates formation of BCN layer on the Cu foil, which is also confirmed by Raman analysis. We explore the anisotropic etching behaviour of the BCN film by annealing in H_2 and Ar atmosphere.

Figure 4a shows an FE-SEM image of the etched BCN structures, where we observed lighter and darker etched areas. We observed growth of overlapped layer structures in the sample, which were simultaneously etched anisotropically. Figure 4b shows a higher

resolution image of the etched BCN structures, where overlapped layer structures can be clearly identify. The additional domains can form on the already grown BCN layer. Figure 4c shows an optical microscope image of the etched BCN layer after transferring to SiO_2/Si substrate. The morphology of etched BCN layers remained intact after the transfer process, which can be also significant for device fabrication. We observed difference in colour contrast of the layers indicating thicker and thinner area, as observed in the SEM image also. Raman study was carried out at various points of the sample to obtain structural information. Figure 4d shows Raman spectra of a micron size BCN sheet after transferring to SiO_2/Si substrate as shown in the optical microscope image. We can observe significant difference than that of pristine or etched graphene structures generally obtained by thermal CVD process using camphor as solid source [31]. A high intensity defect related D band is observed at 1345 cm^{-1}, which is significantly higher than that of G peak (I_D/I_G~2.9, almost three times) at positon 1 of optical microscope image. Again, the graphitic band distinctly split to two peaks with peak centers at 1589 and 1625 $cm^{-1,}$ corresponding to G and G/ peaks. The 2D peak is observed at 2681cm^{-1}, which intensity is almost similar to G peak and much less than D peak. The features of Raman spectra almost similar to the BCN film prior to etching, which signifies incorporation of B and N atoms rather than the edge effect.

The Raman studies confirm formation of highly defective sp^2 hybridized graphene structures on Cu foil. The induced defects with introduction of ammonia borane can be attributed to the incorporation of B and N atoms as detected by XPS analysis. Similarly, we observed defect related D band at 1357 cm^{-1} for overlapped layer structures (position 2 of optical microscope image). The G and 2D peaks were observed at 1584 and 2698 cm^{-1}, respectively. Nevertheless, we observed defects on the top layer, but the bottom layer shows presence of much higher defects. This may be due to less B and N incorporation in the additional domain structures and thereby indicating more of a graphitic nature. Again, we observed a blue-shift (5 cm^{-1}) of the G peak, whereas a red-shift (17 cm^{-1}) for the 2D peak, considering the Si peak as base. Previously, Raman studies of doped graphene have been carried out in details to explain such type of red and blue shift of peak positions, corresponding to doping foreign atoms in graphene lattice [32]. The Raman analysis also provides good evidence of B and N incorporation in crystalline graphene lattice for formation of BCN structures.

Figure 5a shows FE-SEM image of the etched BCN structures on Cu foil. We can observed that the BCN film also etched and formed ribbon-like structures, etched hole and triangular flake as that of graphene and h-BN films. Figure 5b shows formation of

hexagonal hole with pronounced edges as well as hole with more than six edges. There are some overlapped layer structures in the sample, anisotropic etching of these structures occurred simultaneously. Figure 5c shows FE-SEM image of the etched triangular structure interconnected with a ribbon. Figure 5d shows a higher resolution SEM image showing formation of nanoribbon interconnected to two BCN flakes. The width of the NR is around 100 nm. Similarly, figure 5e shows a NR of width ~70 nm connected to an individual BCN sheet. Much thinner NRs can be obtained with control etching conditions for both the h-BN and BCN film. Various other particular structures were also observed by the etching process for the BCN film. Our findings suggest that H_2-induced anisotropic etching of h-BN and BCN basal plane mediated by the SiO_2 nanoparticles can be possible to fabricate NRs and various other structures. The anisotropic etching process can be further exploited to obtain well-ordered NRs by transferring the h-BN and BCN film to Al_2O_3 substrate. As well as, metal nanoparticles assisted etching of h-BN and BCN film can be feasible to obtain particular etched pattern.

4. Conclusions

In summary, we have developed an anisotropic etching process of h-BN and BCN basal plane to fabricate well-defined structures. The anisotropic etching of CVD synthesized h-BN and BCN film on Cu foil was achieved by annealing at 1020 ^{0}C using H_2 (2.5 sccm) and Ar (85 sccm) gas mixture. Formation of h-BN NRs and triangular holes with pronounced edges was observed by the anisotropic etching process. In the etching process, SiO_2 nanoparticles incorporated in the h-BN film on Cu foil during the growth process assisting the H_2-induced etching for the ribbon formation. Similarly, we synthesized BCN layers by mixing camphor and ammonia borane solid precursors as C, N and B source, respectively. Raman studies confirmed B and N atom incorporation in graphene lattice and thereby formation of BCN layers. Anisotropic etching of BCN film was also observed, which creates etched hole and NRs as that of the h-BN layer. The anisotropic etching process of h-BN and BCN basal plane and thereby fabricating NRs and other particular structures can open up new possibilities in 2D hybrid materials fabrication.

Acknowledgements

The work is supported by the funds for the development of human resources in science and technology, Japan.

References

[1] D.B. Lee, J. Appl. Phys. 40 (1969) 4569.

[2] N.C. Lindquist, P. Nagpal, K.M. McPeak, D.J. Norris, S.H. Oh, Rep. Prog. Phys. 75 (2012) 036501.

[3] A.K. Geim, K.S. Novoselov, Nat. Mater. 6 (2007) 183.

[4] K.F. Mak, C. Lee, J. Hone, J. Shan, T.F. Heinz, Phys. Rev. Lett. 105 (2010) 136805.

[5] C.R. Dean, A.F. Young, I. Meric, C. Lee, L. Wang, S. Sorgenfrei, K. Watanabe, T. Taniguchi, P. Kim, K.L. Shepard, J. Hone, Nat. Nanotechnol. 5 (2010) 722.

[6] L.C. Campos, V.R. Manfrinato, J.D. Sanchez-Yamagishi, J. Kong, P. Jarillo-Herrero, Nano Lett. 9 (2009) 2600.

[7] R. Yang, L. Zhang, Y. Wang, Z. Shi, D. Shi, H. Gao, E. Wang, G. Zhang, Adv. Mater. 22 (2010) 4014.

[8] P. S. Fernández, Yoshida K, Ogawa Y, Tsuji M, H. Ago, Adv. Mater. 25 (2013) 6562.

[9] Y. Zhang, Z. Li, P. Kim, L. Zhang, C. Zhou, ACS Nano 6 (2012) 126.

[10] L. Ci, Z. Xu, L. Wang, W. Gao, F. Ding, K.F. Kelly, B.I. Yakobson, P.M. Ajayan, Nano Res. 1 (2008) 116.

[11] P. Nemes-Incze, G. Magda, K. Kamaras, L.P. Biro, Nano Res. 3 (2010) 110.

[12] S.S. Datta, D.R. Strachan, S.M. Khamis, A.T.C. Johnson, Nano Lett. 8 (2008) 1912.

[13] D. Luo, F. Yang, X. Wang, H. Sun, D. Gao, R. Li, J. Yang, Y. Li, Small 10 (2014) 2809

[14] L. Liu , J. Park , D.A. Siegel, K.F. McCarty, K.W. Clark, W. Deng, L. Basile, J.C. Idrobo, A.-P. Li, G. Gu, Science 343 (2014) 343.

[15] G.H. Han, J.A. Rodríguez-Manzo, C.-W. Lee, N.J. Kybert, M.B. Lerner, Z.J. Qi, E.N. Dattoli, A.M. Rappe, M. Drndic, A.T.C. Johnson, ACS Nano 7 (2013) 10129.

[16] S. Sharma, G. Kalita, R. Vishwakarma, Z. Zulkifli, M. Tanemura, Sci. Rep. 5 (2015) 10426.

[17] K. Watanabe, T. Taniguchi, H. Kanda, Nat. Mater. 3 (2004) 404.

[18] K. Watanabe, T. Taniguchi, T. Niiyama, K. Miya, M. Taniguchi, Nat. Photonics 3(2009) 591.

[19] Z. Liu, Y. Gong, W. Zhou, L. Ma, J. Yu, J.C. Idrobo, J. Jung, A.H. MacDonald, R. Vajtai, J. Lou, P.M. Ajayan, Nat. Commun. 4 (2013) 2541.

[20] L. Britnell, R.V. Gorbachev, R. Jalil, B.D. Belle, F. Schedin, A. Mishchenko, T. Georgiou, M.I. Katsnelson, L. Eaves, S.V. Morozov, N.M.R. Peres, J. Leist, A.K. Geim, K.S. Novoselov, L.A. Ponomarenko, Science 335 (2012) 947.

[21] M. Yankowitz, J. Xue, D. Cormode, J.D. Sanchez-Yamagishi, K. Watanabe, T. Taniguchi, P. Jarillo-Herrero, P. Jacquod, B.J. LeRoy, Nat. Phys. 8 (2012) 382.

[22] L. Wang, B. Wu, J. Chen, H. Liu, P. Hu, Y. Liu, Adv. Mater. 26 (2014) 1559.

[23] A. Zhang, H. Teoh, Z. Dai, Y. Feng, C. Zhang, Appl. Phys. Lett. 98 (2011) 023105.

[24] S. Okada, A. Oshiyama, Phys. Rev. Lett. 87 (2001) 146803.

[25] M. Kan, J. Zhou, Q. Wang, Q. Sun, P Jena, Phys. Rev. B 84 (2011) 205412.

[26] V. Barone, J.E. Peralta, Nano Lett. 8 (2008) 2210.

[27] H. Zeng, C. Zhi, Z. Zhang, X. Wei, X. Wang, W. Guo, Y. Bando, D. Golberg, Nano Lett. 10 (2010) 5049.

[28] E.-J. Kan, X. Wu, Z. Li, X.C. Zeng, J. Yang, J.G. Hou, The Jour. Chem. Phys. 129 (2008) 084712.

[29] K.J. Erickson, A.L. Gibb, A. Sinitskii, M. Rousseas, N. Alem, J.M. Tour, A.K. Zettl, Nano Lett. 11 (2011) 3221.

[30] L. Li, L.H. Li, Y. Chen, X.J. Dai, P.R. Lamb, B.M. Cheng, M.Y. Lin, X. Liu, Angew. Chem. 125 (2013) 4306.

[31] A. Thangaraja, S.M. Shinde, G. Kalita, R. Papon, S. Sharma, R. Vishwakarma, K.P. Sharma, M. Tanemura, Appl. Phys. Lett. 106 (2015) 253106.

[32] Z. Zafar, Z.H. Ni, X. Wu, H.N. Shi, H.Y. Nan, J. Bai, L.T. Sun, Carbon 61 (2013) 57.

Figure captions

Figure 1. Optical microscope images of (a) void formation with incomplete growth and (b) continuous h-BN film on Cu foil. XPS spectra of the h-BN film (c) B1s and (d) N1s. (e) AES spectra of as-synthesized h-BN film on Cu foil.

Figure 2 (a) FE-SEM images of etched h-BN film consisting of flakes and etched triangular holes, (b) EDAX analysis of nanoparticle (position 1) on etched h-BN comparing with other part (position 2). FE-SEM image of h-BN (c) nanoribbon (NR) connected to the original h-BN sheet and (d) ribbon-like structure in presence of the SiO_2 nanoparticles. (c) Optical microscope image of etched h-BN layer after transferring to SiO_2/Si substrate.

Figure 3. XPS (a) C1s (BE~284.4 eV), (b) B1s (BE~ 191.2 eV) and (c) N1s (BE~ 398.3 eV) spectra of the BCN film on Cu foil.

Figure 4. FE-SEM image of (a) etched BCN structures, (b) higher resolution image of the etched BCN structures. (c) Optical microscope image of the etched BCN layer after transferring to SiO_2/Si substrate. (d) Raman spectra of the synthesized BCN layers after transferring to SiO_2/Si substrate at positon 1 and 2 as shown in the optical microscope

image.

Figure 5. FE-SEM images of (a) etched BCN structures after the annealing process, (b) formation of hexagonal hole with pronounced edges, (c) etched triangular structure interconnected with a ribbon. Formation of (d) NRs interconnected with two other BCN flakes and (e) NRs connected to an individual BCN sheet.

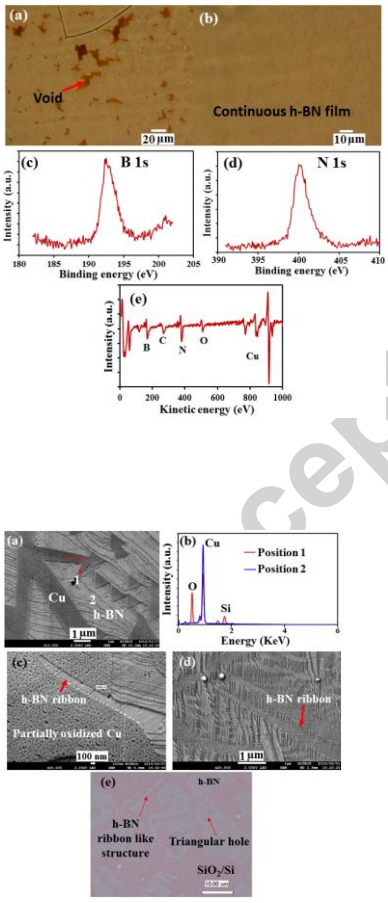

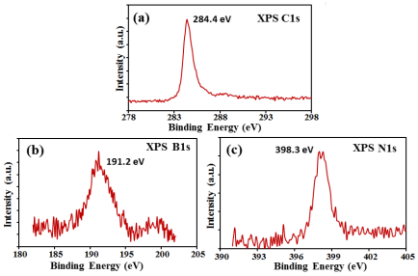

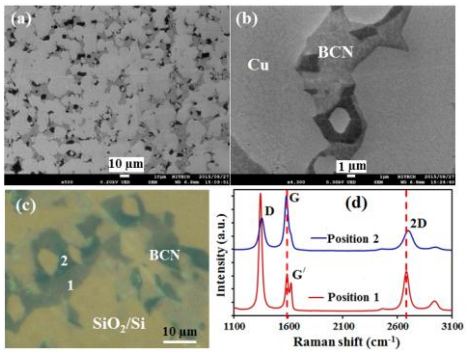

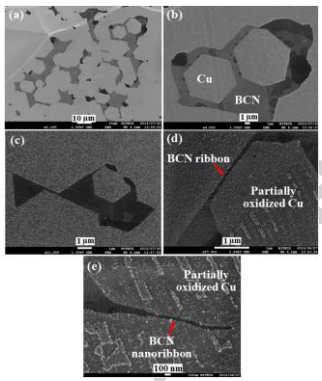

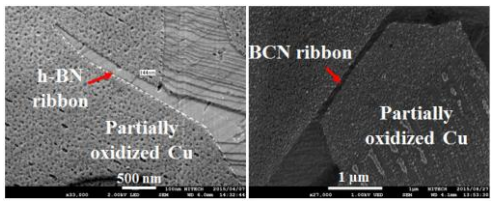

Graphical abstract:

Anisotropic etching of hexagonal boron nitride and boron-carbon-nitrogen layers to fabricate nanoribbons and distinct etched structures by annealing in H_2 and Ar gas mixture.

Highlight

1. Demonstrated anisotropic etching of h-BN for nanoribbons fabrication.
2. Synthesis of BCN layers using mixture of solid sources and their anisotropic etching.
3. Raman studies confirm B and N incorporation in graphene and BCN layer formation.
4. SiO_2 nanoparticles incorporated during growth assisted H_2-induced etching process.
5. The etching process is significant to fabricate various h-BN related novel structures.